PNAS
www.pnas.org

Supplementary Information for

The limits of multifuntionality in tunable networks

Jason W. Rocks, Henrik Ronellenfitsch, Andrea J. Liu*, Sidney R. Nagel, and Eleni Katifori

***To whom correspondence should be addressed. E-mail: ajliu@upenn.edu**

This PDF file includes:

www.pnas.org/cgi/doi/10.1073/pnas.1806790116

Supporting Information Text

Supporting Information (SI)

A. Variations of the network tuning problem. We performed many variations of the standard network tuning problem presented in the main text. The default simulation parameters we used were a pressure (flow networks) or extension (mechanical networks) source, a target relative change in response of $\Delta = 0.1$, and an average node coordination of $Z = 2N_E/N \approx 5.0$. For both flow and mechanical networks, we studied the two cases in which the two source nodes were connected by a single edge and where the two source nodes were chosen randomly from all the nodes, giving 4 cases altogether that we discuss in the main text. Table S1 shows the many variations on these parameters that we explored, along with the resulting power law exponents where applicable and the corresponding figures showing the satisfiability transitions and scaling of the transition position N_T^c and width w. Each set of simulations had at least 128 simulations per data point to calculate the satisfaction probability. The first section of the table shows the data for the four cases discussed in the main text. The second and third sections show configurations for flow and mechanical networks, respectively for higher values of the target relative change Δ. The fourth and fifth sections show results for random networks with $Z \approx 4.1$ (close to isostaticity for mechanical networks) and initially perfect triangular lattices. The sixth section shows configurations for tuning the response with global strains applied to mechanical networks. The seventh section shows results for tuning a target current in response to a current source (flow networks) or target tension in response to a tension source (mechanical networks). Finally, the last two sections show results for a negative relative change in the target response for flow and mechanical networks. All variations on the tuning problem show qualitatively similar power law behavior except for tuning small changes in current or tension (see Section "Tuning target current") or negative desired relative changes in target response, $\Delta < 0.0$) (see Section "Tuning negative target change Δ").

A.1. Tuning target current. In Table S1, we do not list exponents for flow networks tuned for target current nor mechanical networks tuned for target tension with $\Delta = 0.1$. As seen in Figs. S7(A) and (B), these cases do not result in the typical power law behavior seen elsewhere. Instead we find that it is almost always possible to achieve the desired response. This stems from the fact that the current in flow networks or tension in mechanical networks can be trivially increased in magnitude by simply removing the source edge. Typically, the source edge acts as either a resistor or a spring in parallel to the rest of the network, diverting a significant fraction of all current or tension through that edge. If the source edge is removed, then the magnitude of the current or tension is increased without changing the sign. We find that this increase is always enough to satisfy at least a 10% change in magnitude ($\Delta = 0.1$), but not enough to satisfy $\Delta = 1.0$ in flow networks nor $\Delta = 10.0$ in mechanical networks. For these latter cases, the resulting transitions revert back to the typical behavior seen elsewhere.

A.2. Tuning negative target change Δ. The last two sections of Table S1 contain the sets of variables we tested for the alternate case of a negative relative target response, $\Delta < 0$. The resulting transitions are depicted in Figs. S8 and S9. For these cases, we flip the inequality in Eq. (1), resulting in the constraints

$$\frac{\eta_\alpha - \eta_\alpha^{(0)}}{\eta_\alpha^{(0)}} \leq \Delta, \alpha = 1, \ldots, N_T. \quad [1]$$

Note that $\Delta > 0$ corresponds to increasing the magnitude of the response without changing the sign, $-1 < \Delta < 0$ corresponds to decreasing the magnitude of the response without changing the sign, and $\Delta < -1$ corresponds to tuning target responses of the opposite sign from the source. For $\Delta < 0$, we do not always see a simple power law behavior for reasons that are still under investigation.

A.3. Transition in the UK rail network. In order to demonstrate that real transportation networks possess properties similar to those of the jammed packing topologies considered in the main text, we analyze three networks derived from the UK rail network presented in Ref. (1). (i) In Fig. E, we measure P_{SAT} for the full network consisting of $N = 2490$ nodes and $N_E = 4377$ edges for both a node pair source and edge source depicted as blue curves with circular symbols. (ii) While the rail network comprises a single connected component, it contains several parts which are connected through bridges, edges whose removal creates two disconnected components. Because a source located in one such component does not influence any other component, we remove all bridges in the rail network graph and focus on the remaining largest connected component, which consists of $N = 2030$ nodes and $N_E = 3868$ edges. The resulting P_{SAT} curves are shown as the green curves with square symbols in Fig. E. (iii) Within the largest connected component, there are edges whose pressure difference is always zero. For example, such edges may belong to a part of the largest connected component that is connected to the source through only a single node – such a node is topologically equivalent to a bridge. Therefore, we also measure P_{SAT} for the largest connected component where these special edges are excluded from being chosen as targets. The resulting curves are shown in Fig. E in red with triangular symbols. Each case demonstrates decreasing levels of modularity in order from (i) to (iii). In all three cases, we find that the P_{SAT} curves are qualitatively similar to the results we found for networks derived from jammed packings, with increasing modularity resulting in overall lower values of P_{SAT}.

B. Transition power law fitting and deviations. Fig. S11 demonstrates the deviations from power laws for the four systems displayed in Fig. 3. We have plotted the fractional difference of each measured point, N_T^c or w, from its fitted power law function $f(N)$ and $g(N)$, respectively, as a function of system size N. In both cases our fitted function is of the form AN^α where A and α are our fit parameters. Both the data sets for N_T^c and w are fit simultaneously with the same power α, but

different coefficients A, resulting in a total of three fit parameters. Error bars have been estimated by dividing the uncertainty in N_T^c or w by the respective fit function at that point. It is apparent that the simple power law form does not perfectly match the underlying data.

C. Satisfaction probability error bars. Each data point of the various satisfaction probability plots is representative of a binomial distribution

$$p_i \sim \text{Binomial}(n_i, \hat{p}_i) \quad [2]$$

where n_i is the number samples and $\hat{p}_i$ is the fraction of successful tuning attempts. To calculate the error bars depicted in the various satisfaction probability plots, we use the Wilson score interval (2)

$$p_i^{\pm} = \frac{1}{1+\frac{1}{n_i}z^2}\left[\hat{p}_i + \frac{1}{2n_i}z^2 \pm z\sqrt{\frac{1}{n_i}\hat{p}_i(1-\hat{p}_i) + \frac{1}{4n_i^2}z^2}\right] \quad [3]$$

with a z-score of $z = 1$. This gives us an estimate of the uncertainty for each data point which is analogous to the standard deviation for a Gaussian distribution. However, since the probability is restricted between zero and one, the error bars are not necessarily symmetric.

D. Satisfaction probability curve fitting. The satisfaction probability curves depicted in Fig. 2, along with many of the supplemental figures, were estimated using smoothing splines constructed from a basis of cubic B-splines. The procedure for constructing the splines and estimating the smoothing parameter were drawn with some modification from Ref. (3, Chapter 9.2).

To generate an estimate of a satisfaction probability curve, we start with a set of n satisfaction probabilities y_i each generated for a corresponding number of targets x_i where i goes from 1 to n. Each satisfaction probability counts the fraction of successfully tuned networks from a collection of n_i samples. Our goal is to find a function $p(x)$ which approximates the underlying function sampled by the data. Since we do not know what functional form we should use, we would like to approximate this function using a spline. However, the function $p(x)$ should be limited to the interval $[0, 1]$, while splines are not typically limited in this way. Therefore, we write $p(x)$ in terms of a more general function as

$$p(x) = \frac{e^{S(x)}}{1+e^{S(x)}} \quad [4]$$

where $S(x)$ is the spline function which can take on any real value.

D.1. B-spline approximation. In terms of B-splines, the approximating spline function $S(x)$ is written

$$S(x) = \sum_{i=1}^{m} c_i B_i^k(x) \quad [5]$$

with m coefficients c_i and degree-k basis splines $B_i^k(x)$. The coefficients are the fit parameters we would like to estimate.

We must address the specific choices made in the use of B-splines. First, we choose to use cubic splines ($k = 3$). One knot is chosen for each data point plus an extra k at the lowest and highest values of x for padding. This gives us a total of $m = n + 2k$ knots,

$$t_i = \begin{cases} x_1 & \text{if} \quad 0 < i \leq k \\ x_{i-k} & \text{if} \quad k < i \leq n+k \\ x_n & \text{if} \quad n+k < i < n+2k \end{cases} \quad [6]$$

The result is $m = n + 2k - (k + 1)$ basis splines with corresponding coefficients.

D.2. B-spline coefficient estimation. Typically, one would employ a least squares approach to calculate the spline coefficients. However, this assumes that each data point is drawn from some normal distribution, while we know in this case they are drawn from a set of binomial distributions

$$y_i \sim \text{Binomial}(n_i, p(x_i)) \quad [7]$$

Carrying out a standard maximum likelihood estimation, the corresponding log-likelihood of the binomially distributed data is

$$\mathcal{L}(y) = \frac{1}{n}\sum_{i=1}^{n} n_i[y_i \log p(x_i) + (1-y_i)\log(1-p(x_i))] \quad [8]$$

In terms of $S(x)$, the log-likelihood can be written

$$\mathcal{L}(y) = \frac{1}{n}\sum_{i=1}^{n} [b(x_i) - y_i S(x_i)] \quad [9]$$

up to a constant with

$$b(x_i) = n_i \log\left(1 + e^{S(x_i)}\right) \quad [10]$$

To implement smoothing, we introduce a term with penalty parameter λ which penalizes the square of the curvature of $S(x)$. This gives us the penalized generalized linear model

$$I_\lambda(c) = \frac{1}{n}\sum_{i=0}^{n-1}\left[n_i \log\left(1 + e^{S(x_i)}\right) - y_i S(x_i)\right] + \lambda \int_{x_0}^{x_{n-1}} dx[S''(x)]^2 \quad [11]$$

D.3. Smoothing parameter. Next we must choose a good value for λ. This is accomplished using a generalized cross-validation (GCV) approach, allowing us to choose λ in an agnostic manner. Using GCV effectively chooses λ so that the approximating spline curve changes as little as possible if an arbitrary subset of data is left out of the fit. For the sake of convenience, we write

$$S(x) = \langle c|B^k(x)\rangle \quad [12]$$

where $c_i = \langle i|c\rangle$ and $B_i^k(x) = \langle i|B^k(x)\rangle$ are vectors of size m. We also write

$$\Sigma_{ij} = \int_{x_0}^{x_{n-1}} dx B_i^k(x) B_j^k(x) \quad [13]$$

Finally, we minimize the generalized cross-validation function

$$V(\lambda)_{GCV} = \frac{\sum_{i=1}^{n}\left[D_i^{-\frac{1}{2}}(y_i - \mu_i)\right]^2}{\frac{1}{n}\,\mathrm{tr}^2(I - A)} \quad [14]$$

with

$$\mu_i = b'(S(x_i)) \quad [15]$$

$$D_i = b''(S(x_i)) \quad [16]$$

and

$$A_{ij} = D_i^{\frac{1}{2}} \langle B^k(x_i)| \left[\sum_{l=1}^{n} D_l |B^k(x_l)\rangle\langle B^k(x_l)| + 2\lambda\Sigma\right]^{-1} |B^k(x_j)\rangle D_j^{\frac{1}{2}} \quad [17]$$

The size $n \times n$ matrix I is the identity. When testing a particular value of λ, the values c_i are always chosen to minimize Eq. (11) for that λ. Therefore, the spline coefficients are treated as a function of λ.

When minimizing Eq. (14), there may sometimes be extraneous minima at $\lambda = 0$ or $\lambda = \infty$. Since we would like some degree of smoothing, we never choose the minimum at zero. Also, moderate smoothing is generally preferable to infinite smoothing, so if a local minimum exists for finite λ, it is chosen even if it is not the global minimum.

E. Transition measurements. We use the spline approximations of each satisfaction probability curve in order to estimate the positions and widths of each satisfiability transition. The center of the transition is simply chosen as the number of targets N_T^c such that the probability of success is exactly 50%, $P_{SAT}(N_T^c) = 0.5$. The width of the transition w is found by first finding the number of targets corresponding to success rates of 25% and 75% and taking their differences, $w = P_{SAT}^{-1}(0.75) - P_{SAT}^{-1}(0.25)$. In order to weight each point correctly when finding the power law scaling of the transition properties, we utilized Monte Carlo resampling to estimate uncertainty (4). To find the uncertainty values for N_T^c and w for a particular curve, each data point for that curve is resampled from its underlying binomial distribution. The spline approximation is then recalculated for this new set of data points and new values of N_T^c and w are extracted. This process is repeated numerous times, resulting in a distribution of value of N_T^c and w. The uncertainty is then calculated by finding the standard deviation of of these distributions.

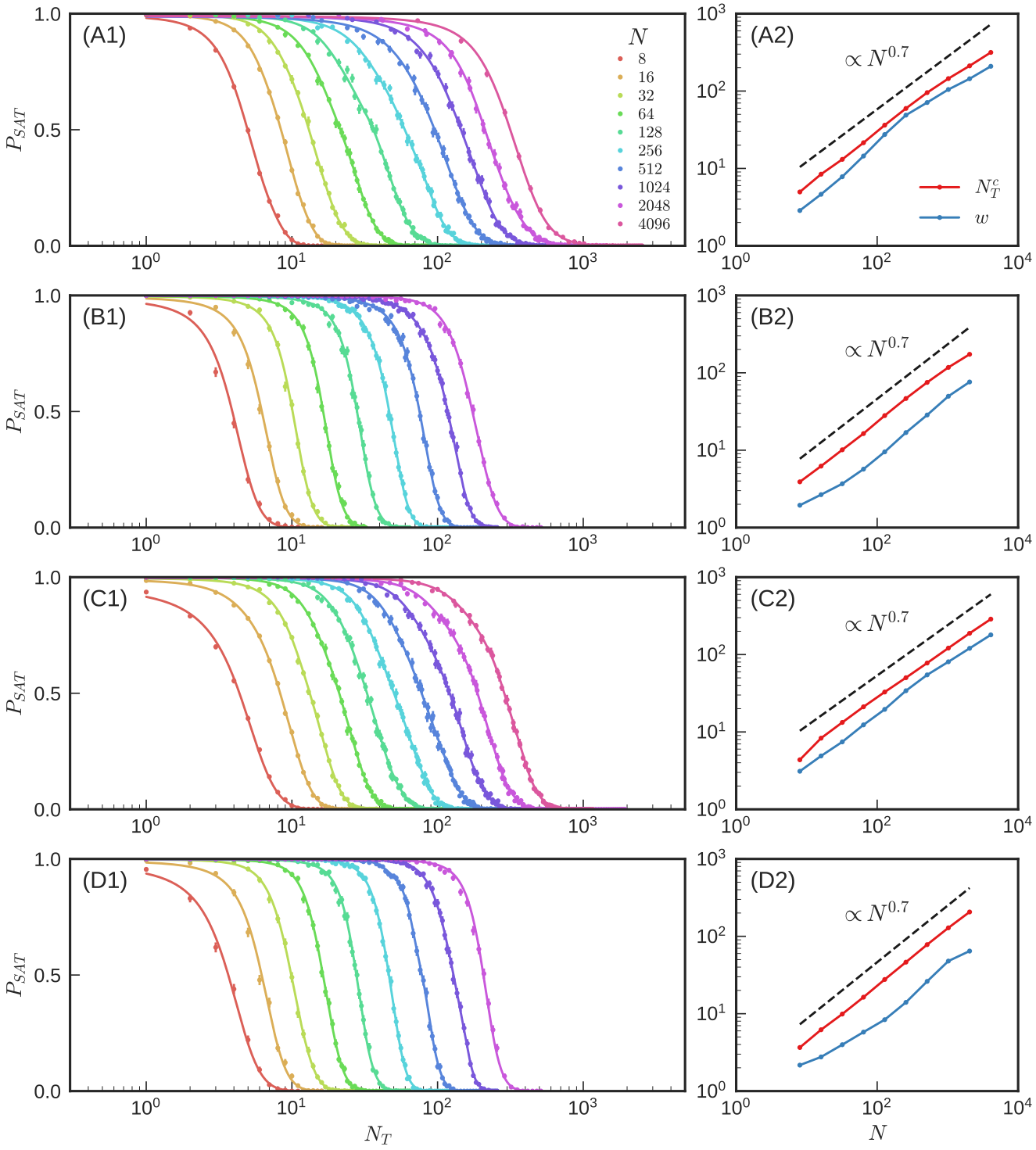

Fig. S1. Satisfaction probability and scaling of the transition position and width for the four main cases shown in the main text: (A) flow networks and (B) mechanical networks with an edge source and (C) flow networks and (D) mechanical networks with a node pair source. See Table S1 for more details.

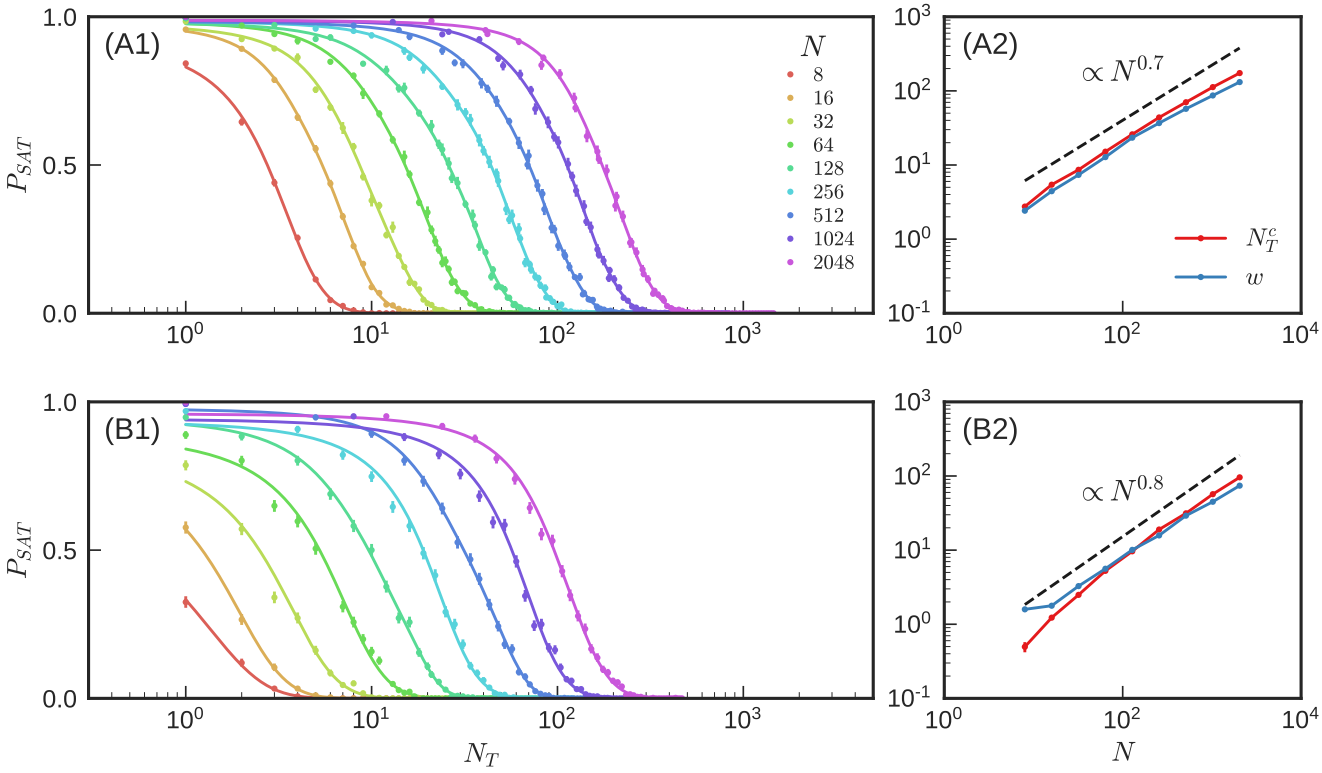

Fig. S2. Satisfaction probability and scaling of the transition position and width for flow networks with desired relative change in target response of (A) $\Delta = 1.0$ and (B) $\Delta = 10.0$. See Table S1 for more details.

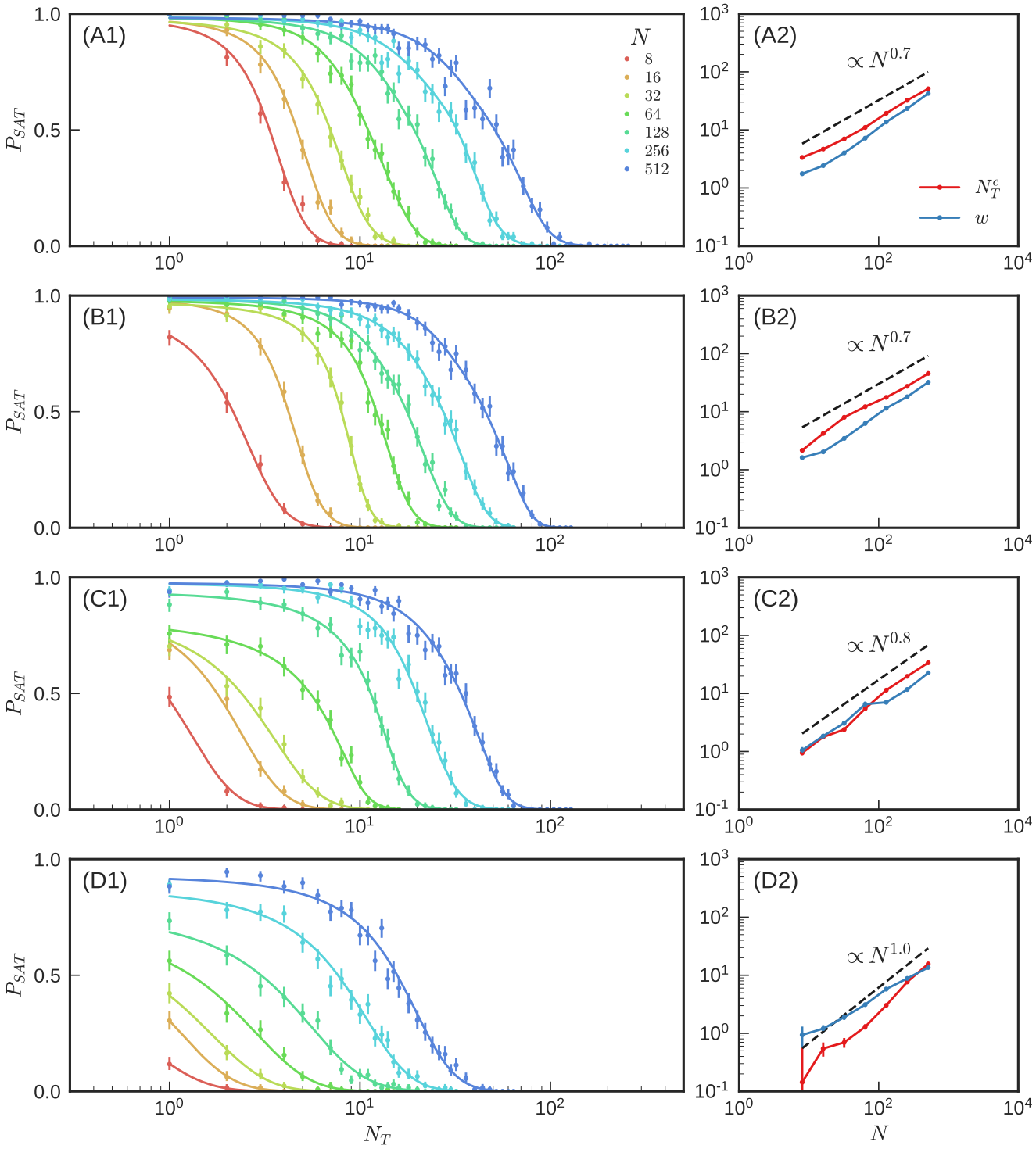

Fig. S3. Satisfaction probability and scaling of the transition position and width for mechanical networks with desired relative change in target response of (A) $\Delta = 1.0$, (B) $\Delta = 10.0$, (C) $\Delta = 100.0$, and (D) $\Delta = 1000.0$. See Table S1 for more details.

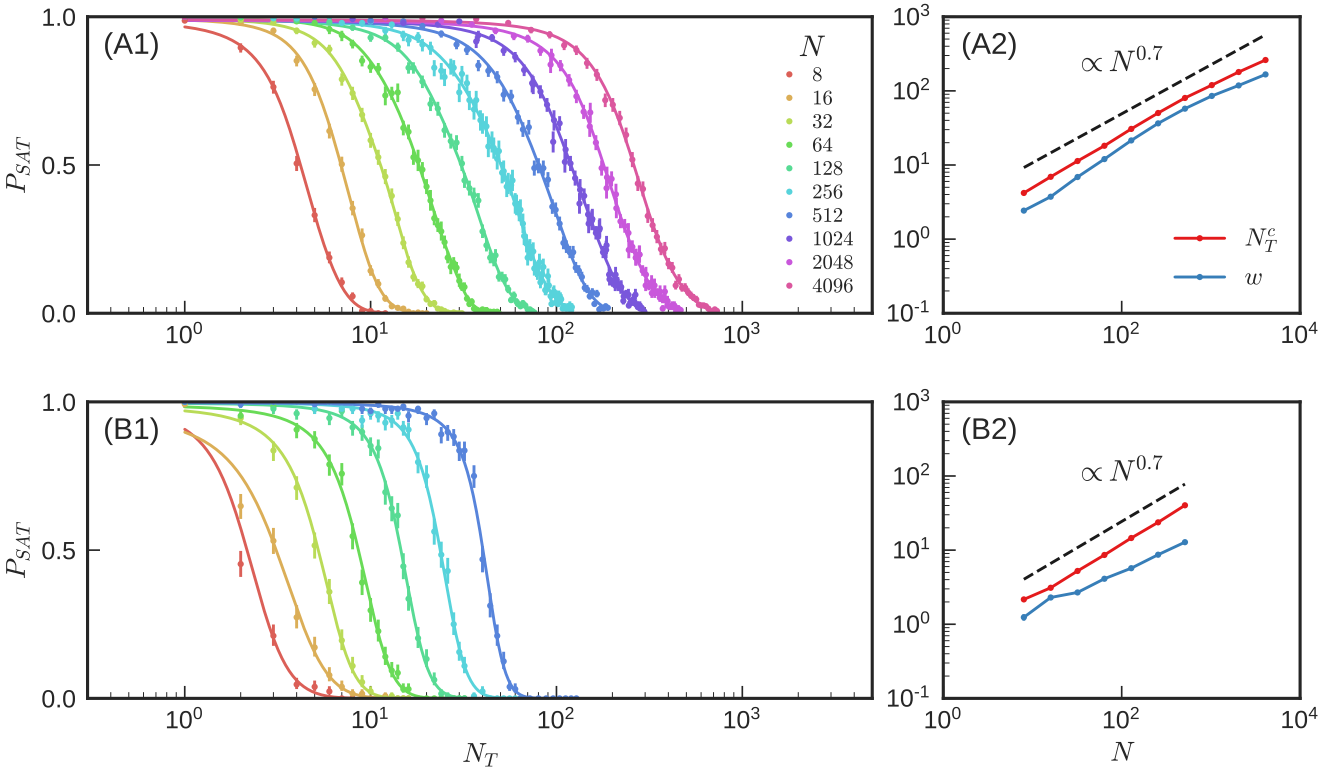

Fig. S4. Satisfaction probability and scaling of the transition position and width for (A) flow networks and (B) mechanical networks with average connectivity of $Z \approx 4.1$, lower than the default of $Z \approx 5.0$. See Table S1 for more details.

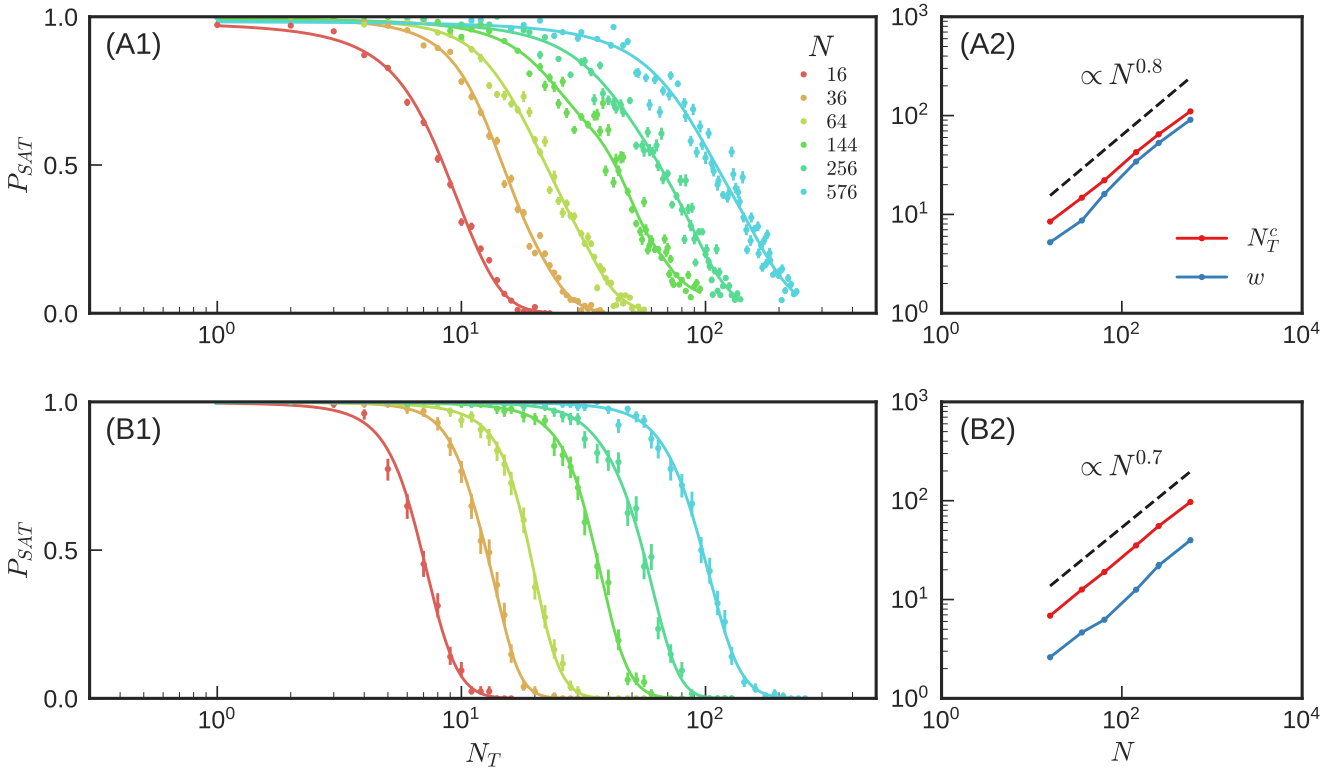

Fig. S5. Satisfaction probability and scaling of the transition position and width for (A) flow networks and (B) mechanical networks on an ordered triangular lattice. See Table S1 for more details.

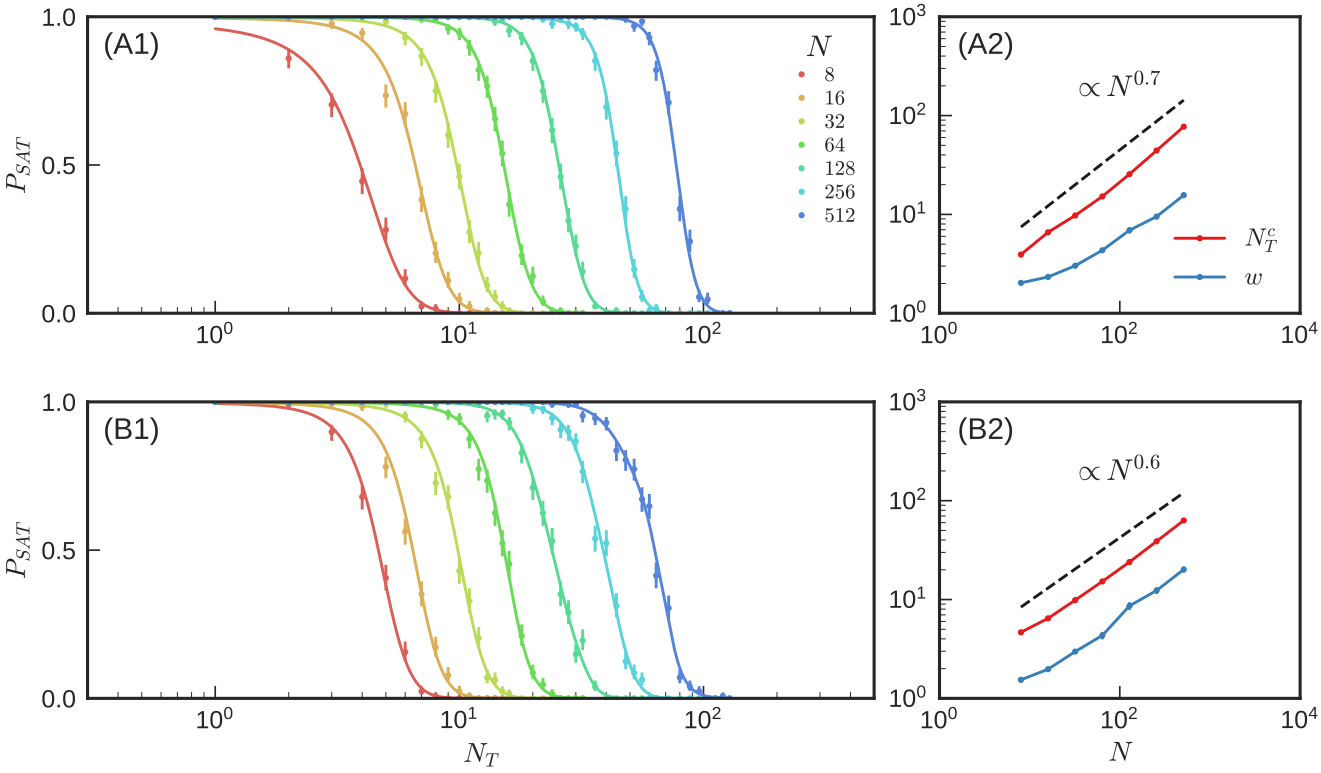

Fig. S6. Satisfaction probability and scaling of the transition position and width for mechanical networks with global (A) shear and (B) compression sources. See Table S1 for more details.

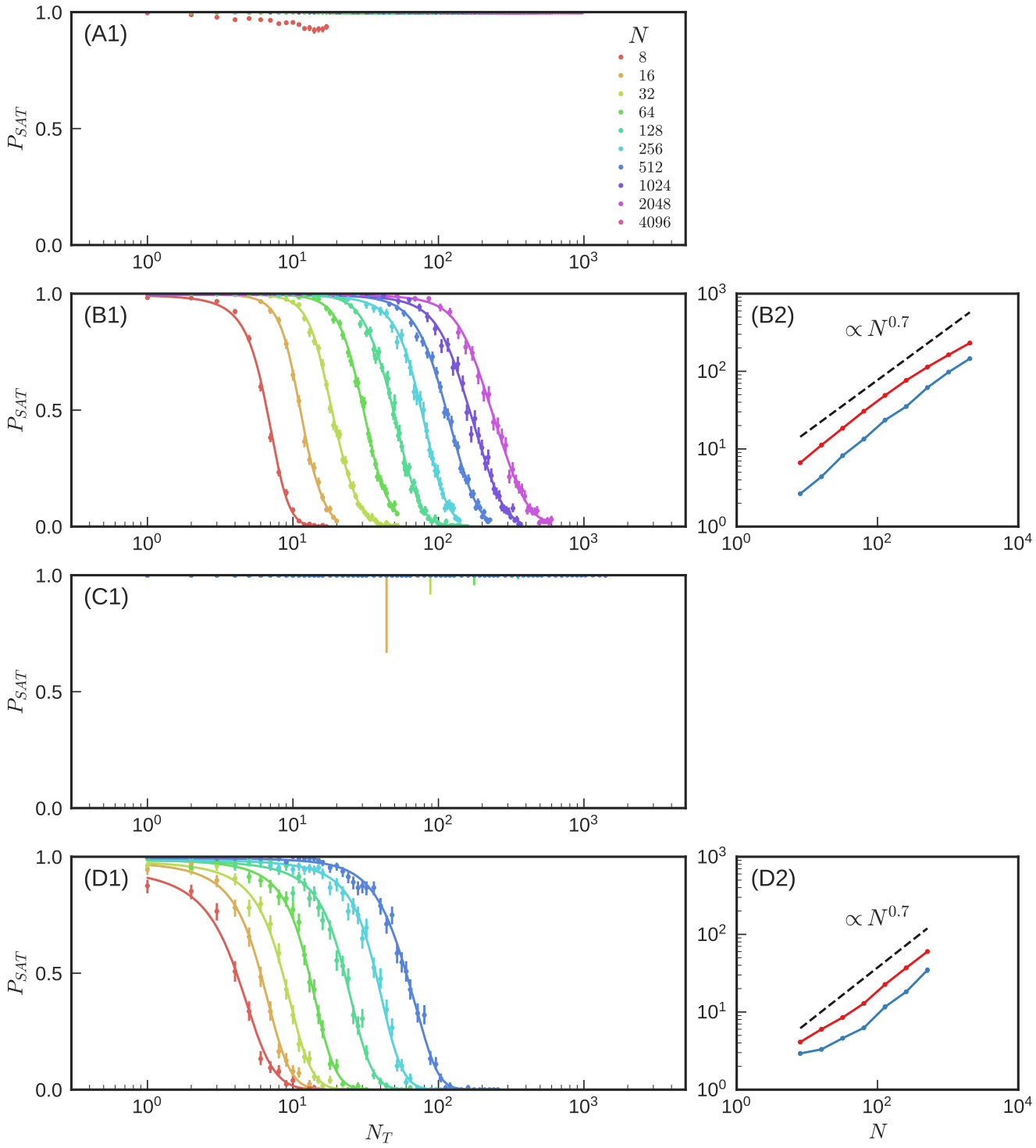

Fig. S7. Satisfaction probability and scaling of the transition position and width for flow networks tuned for target current with (A) $\Delta = 0.1$ and $\Delta = 1.0$ and mechanical networks tuned for target tension with (C) $\Delta = 0.1$ and (D) $\Delta = 10.0$. See Table S1 for more details. Large error bars reflect a lack of available networks with enough edges to measure P_{SAT} for large N_T.

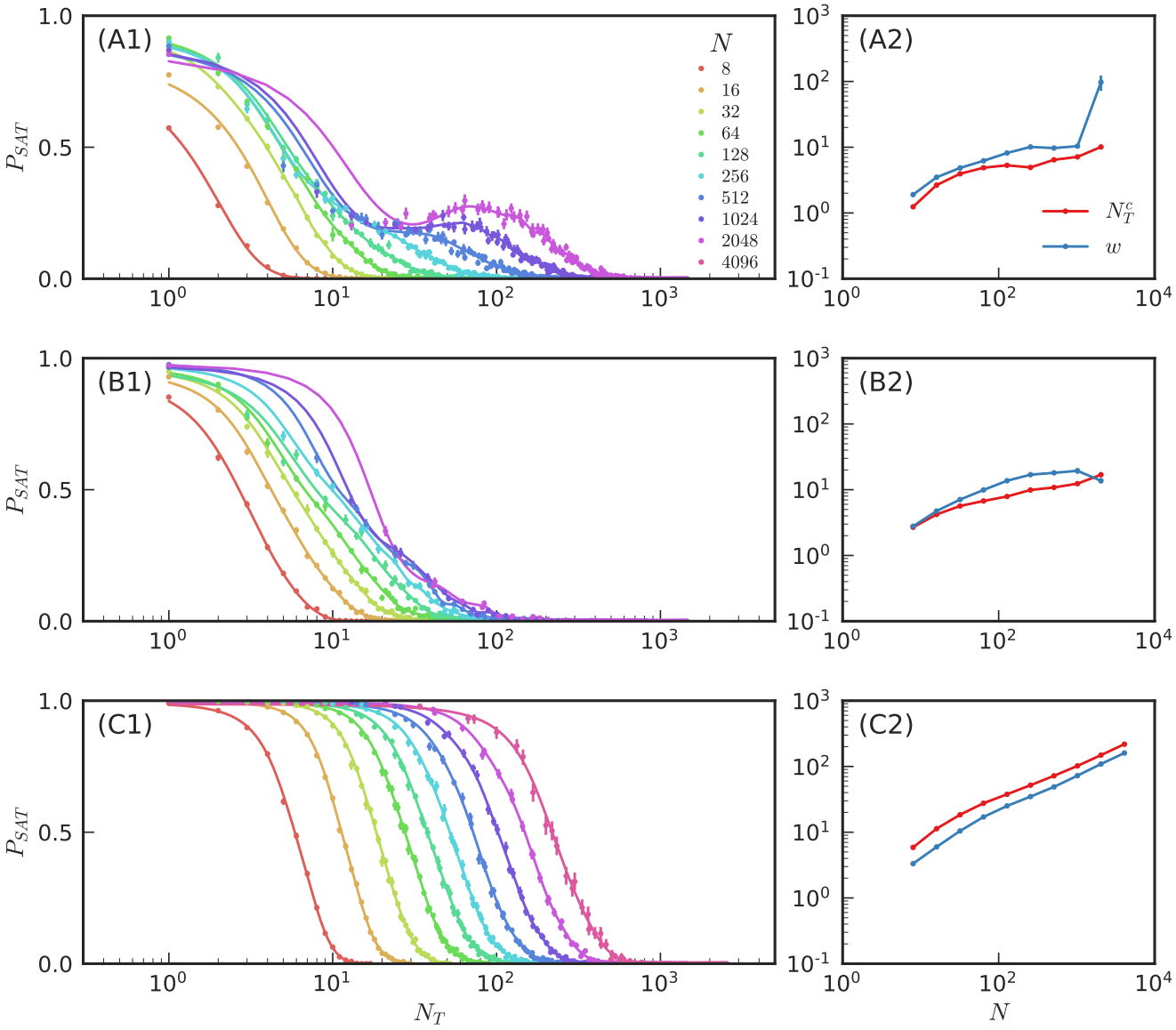

Fig. S8. Satisfaction probability and scaling of the transition position and width for flow networks tuned for a negative relative change in target response of (A) $\Delta = -0.5$, (B) $\Delta = -1.0$, and (C) $\Delta = -1.5$. See Table S1 for more details.

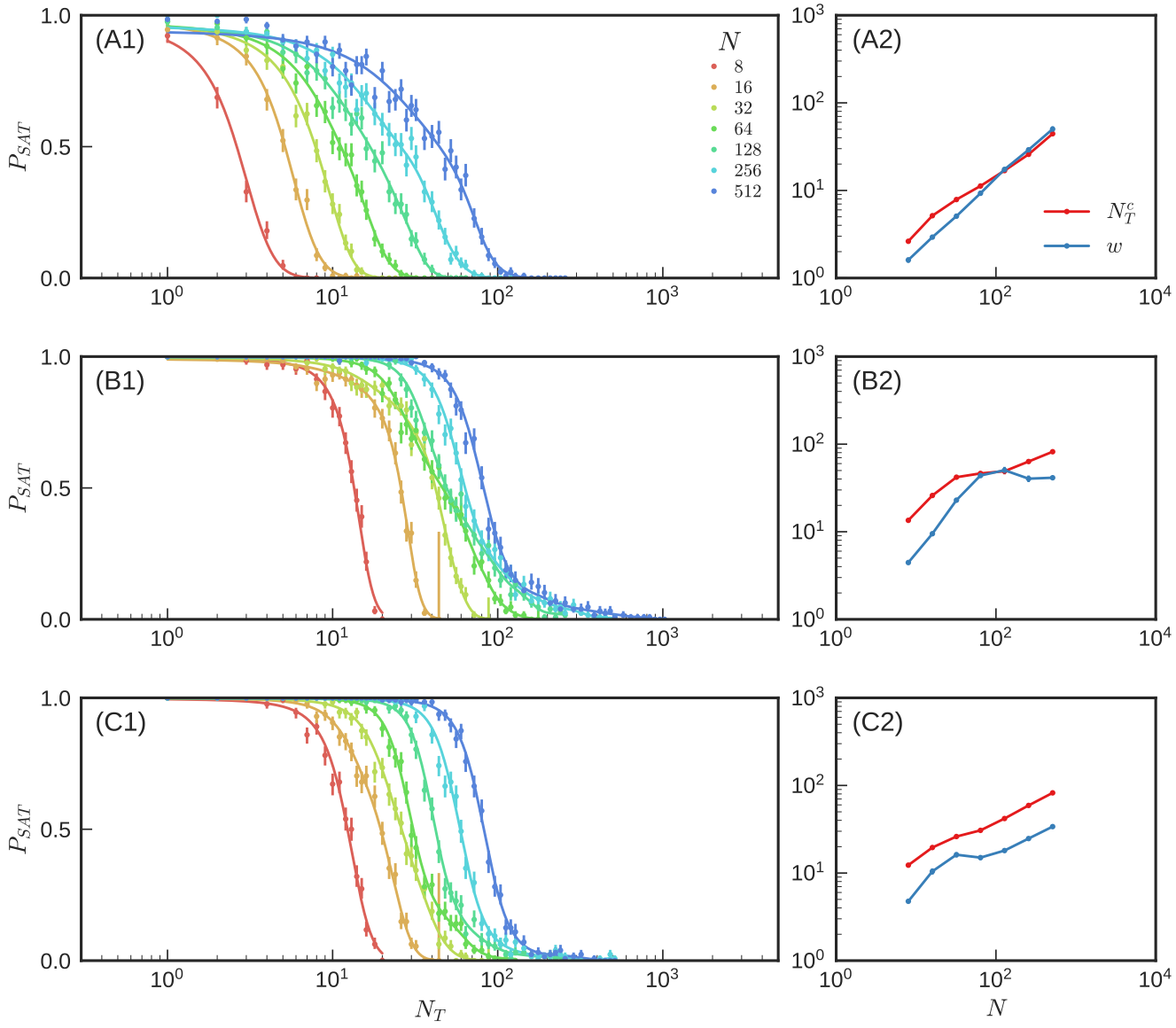

Fig. S9. Satisfaction probability and scaling of the transition position and width for mechanical networks tuned for a negative relative change in target response of (A) $\Delta = -0.5$, (B) $\Delta = -1.0$, and (C) $\Delta = -1.5$. See Table S1 for more details. Large error bars reflect a lack of available networks with enough edges to measure P_{SAT} for large N_T.

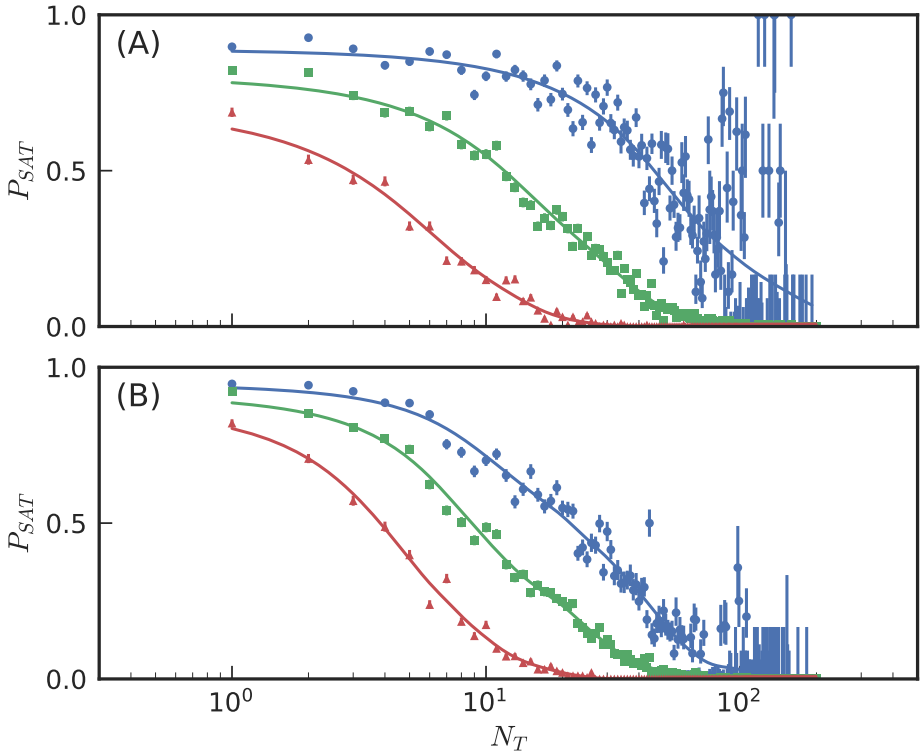

Fig. S10. Satisfaction probability of flow networks derived from real UK railroad networks with (A) an edge source and (B) a node pair source. Three cases are shown for each source: (blue curves with circular symbols) The entire network is used. (green curves with square symbols) All bridge edges are removed and only the largest connected component is used. (red curves with triangular symbols) The largest connected component is used and edges whose pressure differences will always be zero are excluded from being chosen as targets. See Section A.3 for more details.

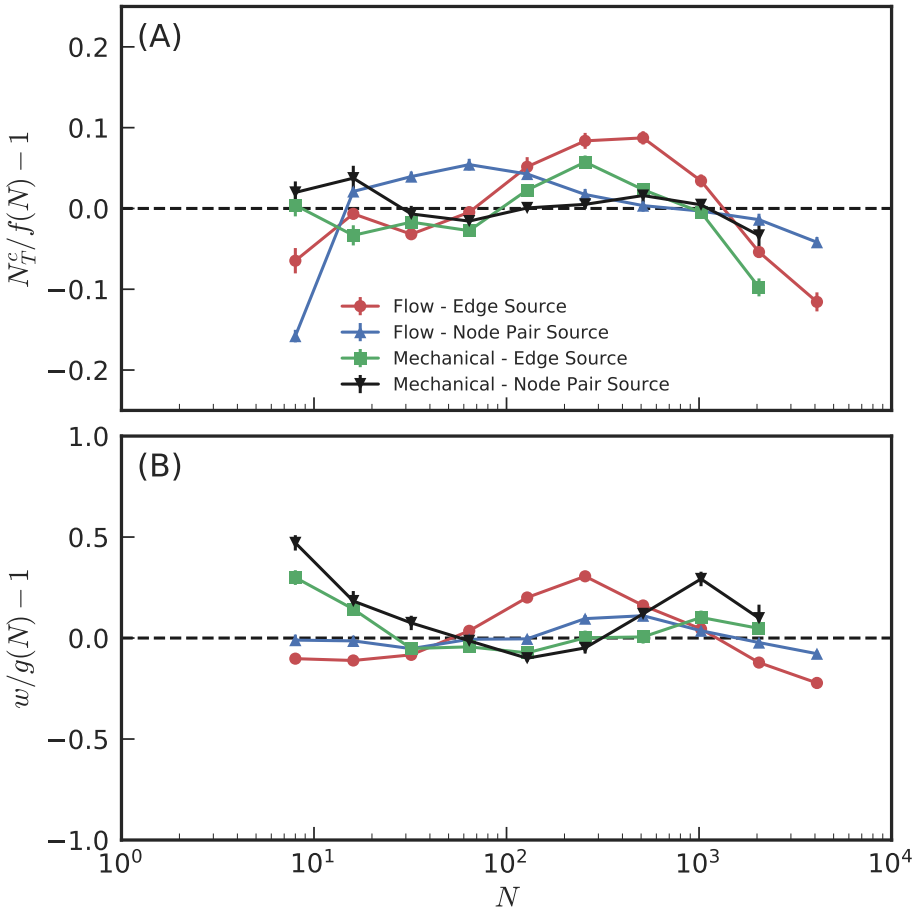

Fig. S11. Deviations of the power laws in Fig. 3 of the main text from power laws of the form $f(N) = AN^{\alpha}$ for the transition position and $g(N) = BN^{\alpha}$ for the transition width. Error bars for the position and width have been rescaled by dividing by $f(N)$ or $g(N)$, respectively.

Table S1. Variations of tuning problem and corresponding transition exponents

Physical System	Source Properties	Target Properties	Target Change Δ	Network Properties	Transition Position Exponent ν	Figure(s)
Flow	Edge Pressure Drop	Edge Pressure Drop	0.1	Random - $Z \approx 5.0$	0.7	1(A), 2(A),3, S1(A)
Mechanical	Edge Extension	Edge Extension	0.1	Random - $Z \approx 5.0$	0.7	1(B), 2(B), 3, S1(B)
Flow	Node Pair Pressure Drop	Edge Pressure Drop	0.1	Random - $Z \approx 5.0$	0.7	1(C) 3, S1(C)
Mechanical	Node Pair Extension	Edge Extension	0.1	Random - $Z \approx 5.0$	0.7	1(D) 3, S1(D)
Flow	Edge Pressure Drop	Edge Pressure Drop	$\mathbf{1.0}$	Random - $Z \approx 5.0$	0.7	S2(A)
Flow	Edge Pressure Drop	Edge Pressure Drop	$\mathbf{10.0}$	Random - $Z \approx 5.0$	0.8	S2(A)
Mechanical	Edge Extension	Edge Extension	$\mathbf{1.0}$	Random - $Z \approx 5.0$	0.7	S3(A)
Mechanical	Edge Extension	Edge Extension	$\mathbf{10.0}$	Random - $Z \approx 5.0$	0.7	S3(B)
Mechanical	Edge Extension	Edge Extension	$\mathbf{100.0}$	Random - $Z \approx 5.0$	0.8	S3(C)
Mechanical	Edge Extension	Edge Extension	$\mathbf{1000.0}$	Random - $Z \approx 5.0$	1.0	S3(D)
Flow	Edge Pressure Drop	Edge Pressure Drop	0.1	**Random - Z** $\approx \mathbf{4.1}$	0.7	S4(A)
Mechanical	Edge Extension	Edge Extension	0.1	**Random - Z** $\approx \mathbf{4.1}$	0.7	S4(B)
Flow	Edge Pressure Drop	Edge Pressure Drop	0.1	**Triangular Lattice**	0.8	S5(C)
Mechanical	Edge Extension	Edge Extension	0.1	**Triangular Lattice**	0.7	S5(D)
Mechanical	**Global Shear**	Edge Extension	0.1	Random - $Z \approx 5.0$	0.7	S6(A)
Mechanical	**Global Expansion**	Edge Extension	0.1	Random - $Z \approx 5.0$	0.6	S6(B)
Flow	Edge Current	**Edge Current**	0.1	Random - $Z \approx 5.0$	N/A	S7(A)
Flow	Edge Current	**Edge Current**	$\mathbf{1.0}$	Random - $Z \approx 5.0$	0.7	S7(B)
Mechanical	Edge Tension	**Edge Tension**	0.1	Random - $Z \approx 5.0$	N/A	S7(C)
Mechanical	Edge Tension	**Edge Tension**	$\mathbf{10.0}$	Random - $Z \approx 5.0$	0.7	S7(D)
Flow	Edge Pressure Drop	Edge Pressure Drop	$\mathbf{-1.5}$	Random - $Z \approx 5.0$	N/A	S8(A)
Flow	Edge Pressure Drop	Edge Pressure Drop	$\mathbf{-1.0}$	Random - $Z \approx 5.0$	N/A	S8(B)
Flow	Edge Pressure Drop	Edge Pressure Drop	$\mathbf{-0.5}$	Random - $Z \approx 5.0$	N/A	S8(C)
Mechanical	Edge Extension	Edge Extension	$\mathbf{-1.5}$	Random - $Z \approx 5.0$	N/A	S9(A)
Mechanical	Edge Extension	Edge Extension	$\mathbf{-1.0}$	Random - $Z \approx 5.0$	N/A	S9(B)
Mechanical	Edge Extension	Edge Extension	$\mathbf{-0.5}$	Random - $Z \approx 5.0$	N/A	S9(C)

N/A indicates power law estimates not applicable due to lack of transition, or clearly non-power-law-like behavior.
Bold text indicates changes from default parameters.

References

1. Gallotti R, Barthelemy M (2015) The multilayer temporal network of public transport in Great Britain. *Sci Data* 2:140056.
2. Wilson EB (1927) Probable inference, the law of succession, and statistical inference. *J Am Stat Assoc* 22(158):209–212.
3. Wahba G (1990) *Spline Models for Observational Data.* (Society for Industrial and Applied Mathematics).
4. Press WH (2007) *Numerical Recipes 3rd Edition: The Art of Scientific Computing.* (Cambridge University Press).